Mon. Not. R. astr. Soc. (1986) **218,** 761–773

Emission line formation in accretion discs

Keith Horne* and T. R. Marsh *Institute of Astronomy, Madingley Road, Cambridge CB3 0HA*

Accepted 1985 September 10. Received 1985 September 4; in original form 1984 December 28

Summary. We examine the formation of emission lines from accretion discs and develop simple expressions for computing the profiles of both optically thin and optically thick lines. The effect of the Keplerian velocity gradient on the transfer of line radiation in the disc is taken into account to first order in H/R. Line photons that are trapped in an optically thick emission layer can escape more easily in directions along which the Keplerian shear flow provides large Doppler gradients. This anisotropy in the local emission pattern alters the shape of the global emission line profile. We present synthetic emission line profiles for the optically thick and optically thin limits and covering a full range of inclinations. The resemblance between our high-inclination optically thick line profiles and the observed profiles of Balmer emission lines in eclipsing dwarf novae indicates that this local saturation effect is an important element of the line formation process in real discs.

1 Introduction

The optical spectra of many cataclysmic variables display strong Balmer, He I, and He II emission lines (see for example Williams 1983). The velocity profiles of the lines provide a means of investigating the dynamics of these short-period binaries and the accretion flows between their red dwarf and white component stars. Linewidths of several thousand kilometres per second and double-peaked line profiles associate the emission lines with the accretion disc that surrounds the white dwarf. The emission lines are eclipsed by the red dwarf star in systems that are viewed at a large inclination. In such cases the eclipse of the blue side of the emission line precedes that of the red side (Greenstein & Kraft 1959; Young, Schneider & Shectman 1981b), demonstrating explicitly that the emission line gas occupies an extended region and that it rotates about the white dwarf in the expected prograde direction. Such observations firmly establish that most of the optical line emission originates in the disc.

In the steady-state accretion disc models developed by Williams (1980) and Tylenda (1981), Balmer emission lines are produced in LTE by an outer disc region that is transparent in the Paschen continuum but opaque in the lines. The low free–free and free–bound continuum

*Now at the Space Telescope Science Institute, Homewood Campus, The Johns Hopkins University, Baltimore, MD 21218, USA.

opacity in the outer disc results from the predominantly neutral condition of hydrogen at the low temperatures ($T \lesssim 7000$ K) that are present there. A second possible source of line emission is a disc chromosphere, which may be heated by a vertical transport of energy (Liang & Price 1977) or by hard radiation from the vicinity of the central object (Jameson, King & Sherrington 1980; Schwarzenberg-Czerny 1981; Elitzer *et al.* 1983). Analyses of the observed line profiles, of eclipse phenomena, and of rapid time variations are needed to clarify the roles played by these two mechanisms in forming the emission lines.

The line formation problem in accretion discs divides naturally into two parts. A local radiative transfer problem first defines the spectral and angular distribution of the radiation emerging from each point on the disc surface. The global line profile then is assembled by summing the independent contributions from each part of the disc surface, with appropriate Doppler shifts to account for the orbital motion of the disc material. As the orbital velocities in a thin accretion disc are highly supersonic, the local line profile widths generally are much smaller than the orbital Doppler widths. Consequently, it has been possible without considering the local radiative transfer problem in detail to account for the double-peaked morphology of the emission lines (Smak 1969; Huang 1972) and to interpret the shape of the emission line wings in terms of a simple line emissivity distribution $j(R)$ defined on the surface of the disc (Smak 1981; Stover 1981; Young *et al.* 1981b).

Flat decrements imply that the Balmer emission lines in cataclysmic variable stars are optically thick. For such lines the local line emissivity must be strongly anisotropic, since line photons trapped in an optically thick emission layer can emerge more readily in directions along which the Keplerian velocity field provides a large Doppler shift gradient. Thus, despite its successes, the description of line emission in terms of a simple isotropic line emissivity probably is incorrect.

The supersonic orbital velocities present in a thin disc have motivated a use of the Sobolev approximation in computing profiles for optically thick emission lines from discs. Gorbatskii (1965) presents analytical results for the wings of optically thick emission lines from an edge-on disc. Rybicki & Hummer (1983) consider a thin Keplerian disc to illustrate their general formalism for treating the transfer of radiation in moving three-dimensional media. Their line profiles, computed in the Sobolev approximation for a narrow disc annulus ($\Delta R/R \ll 1$), range from the familiar 'U-shaped' profile in the optically thin case to 'M-shaped' profiles for optically thick lines. These results clearly demonstrate the importance of local radiative transfer effects. Rybicki & Hummer indicate, however, that the velocity gradient in a Keplerian disc is only marginally large enough to justify use of the Sobolev theory.

The aim of our paper is to illustrate the physical processes that shape the profiles of emission lines from discs, and to derive some expressions that may be used to interpret the observed profiles of both optically thin and optically thick lines. Rather than adhering to a rigorous treatment of the local radiative transfer problem, we employ several approximations that capture the basic features of the problem and allow us to arrive at analytical results. Our presentation parallels the historical development of the subject. We first treat in Section 2 the origin of double-peaked line profiles and the connection between the emission distribution on the disc surface and the profile of the emission line wings. We then turn in Section 3 to the local radiative transfer problem, emphasizing the role played by the Keplerian shear in determining the angular distribution of line photons emerging from an optically thick emission layer. Section 4 presents synthetic profiles for optically thick and thin emission lines over a full range of inclinations and discusses some implications of our results.

2 The assembly of disc line profiles

Emission lines from accretion discs are broadened primarily by Doppler shifts due to orbital motion of the material in the disc around the massive object at its centre. Material at radius R in a

physically thin disc around an object of mass M moves approximately in a circular orbit with the Keplerian speed

$$V_{\rm Kep}=\left(\frac{GM}{R}\right)^{1/2}. \tag{1}$$

For a distant observer, the Doppler velocity shift produced by this orbital motion is

$$V_{\rm D}=V_{\rm Kep}\sin i\sin\theta, \tag{2}$$

where i is the inclination angle between the observer's line-of-sight and the direction normal to the disc plane, and θ is the azimuth angle relative to the line-of-sight, or equivalently the azimuth of the observer relative to the radius vector of the disc material.

The disc's global emission line profile is assembled by summing the independent Doppler-shifted contributions from each part of the accretion disc surface:

$$F_\nu=\int\frac{R\,dR\,d\theta}{D^2}f_\nu. \tag{3}$$

Here D is the distance to the system, and the local line profiles f_ν each are shifted from the rest frequency ν_0 to the local Doppler frequency

$$\nu_{\rm D}=\nu_0\left(1-\frac{V_{\rm D}}{c}\right). \tag{4}$$

In the simple formalism that up to now has been used to interpret observations of emission lines from accretion discs, the local line profile f_ν is expressed as

$$f_\nu=j(R)\phi_\nu, \tag{5}$$

where $\int\phi_\nu\,d\nu=1$. The shape of the normalized local line profile ϕ_ν has little effect on the global line profile provided its velocity width, of the order of the local sound speed, is small in comparison with the orbital velocities. The local line emissivity $j(R)$ in equation (5) is implicitly assumed to be axisymmetric and isotropic.

In the remainder of this section we examine the interpretation of emission lines from discs in the context of these assumptions. We shall see in the following section how the assumed isotropy of J is modified for optically thick lines.

2.1 THE ORIGIN OF DOUBLE-PEAKED PROFILES

The origin of double-peaked emission line profiles from accretion discs is illustrated in Fig. 1. The 'dipole field' pattern that is traced out by loci of constant radial velocity on the face of a Keplerian disc is shown in Fig. 1(a). The disc's global emission line profile, shown in Fig. 1(b), is divided into velocity bins corresponding to the disc regions between consecutive dipole field lines.

The emission in each velocity bin thus arises from a different region of the disc surface. Material on the front-to-back bisector of the disc ($\theta=0,\pi$) moves in a direction perpendicular to the line-of-sight and gives rise to emission at the centre of the line profile ($V=0$). Velocity bins in the wings of the line profile stem from small crescent-shaped regions close to the central object. The area of the disc surface contained within each such crescent is proportional to $R\,\Delta R$, since $R\propto V^{-2}$ in a Keplerian disc, to $V^{-5}\,\Delta V$. It is mainly this rapid reduction in surface area with increasing V that is responsible for the declining emission in the wings of the line profile.

The transition from a complete crescent to one that is truncated at the outer radius $R_{\rm D}$ produces cusps in the line profile at $V_{\rm D}=\pm V_{\rm Kep}(R_{\rm D})\sin i$. Double-peaked line profiles thus reflect the existence of an outer boundary to the emission line region.

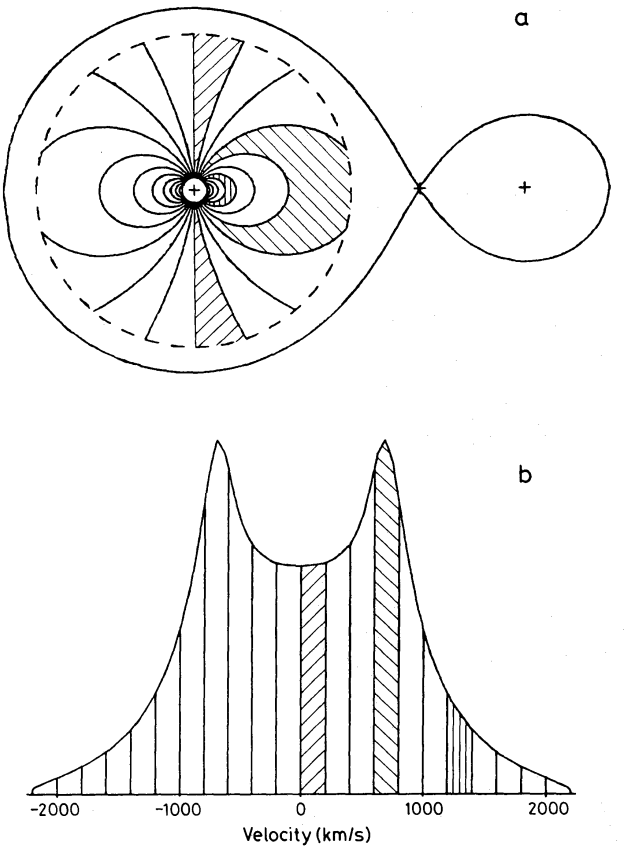

Figure 1. (a) A Keplerian accretion disc in a binary of mass ratio $q=0.15$ is viewed at quadrature. The loci of constant radial velocity form a dipole field pattern on the surface of the disc. (b) The velocity profile of emission lines from the disc. Emission in the shaded velocity bins arises from the corresponding regions of the disc.

2.2 THE LINE SURFACE BRIGHTNESS AND EMISSION IN THE WINGS

Most attempts to model the profiles of emission lines from discs (Young & Schneider 1980; Smak 1981; Stover 1981; Clarke, Capel & Bowyer 1985) have assumed a power-law model of the form

$$j(R) \propto R^{-b}. \tag{6}$$

Fig. 2 presents a series of synthetic emission line profiles for a range of power-law exponents, together with the observed Hα profile of the eclipsing dwarf nova Z Cha ($i=82°$). A power-law model with exponent $b=1.7$ matches the wings of the observed profile. The peaks of the model profile are too sharp, however, and the U-shaped valley separating them appears to be of insufficient depth.

The observed profile, an average over two 107-min binary orbits, was obtained with the IPCS detector at the Anglo-Australian Telescope. Other eclipsing dwarf novae, e.g. HT Cas (Young *et al.* 1981b) and OY Car (Schoembs & Hartman 1984), exhibit similar emission line profiles. We have chosen the Hα profile in order to minimize contamination by photospheric absorption lines from the white dwarf at the centre of the disc. (The white dwarf lines become more prominent higher up in the Balmer series, where broad absorption wings flank the double-peaked emission lines and the central absorption in some cases dips below the level of the interpolated continuum.) Eclipse behaviour indicates that the white dwarf lines may contribute at most 10 per cent to the depth of the valley between the emission peaks. Our observations of Z Cha are discussed in more detail elsewhere (Marsh & Horne 1985).

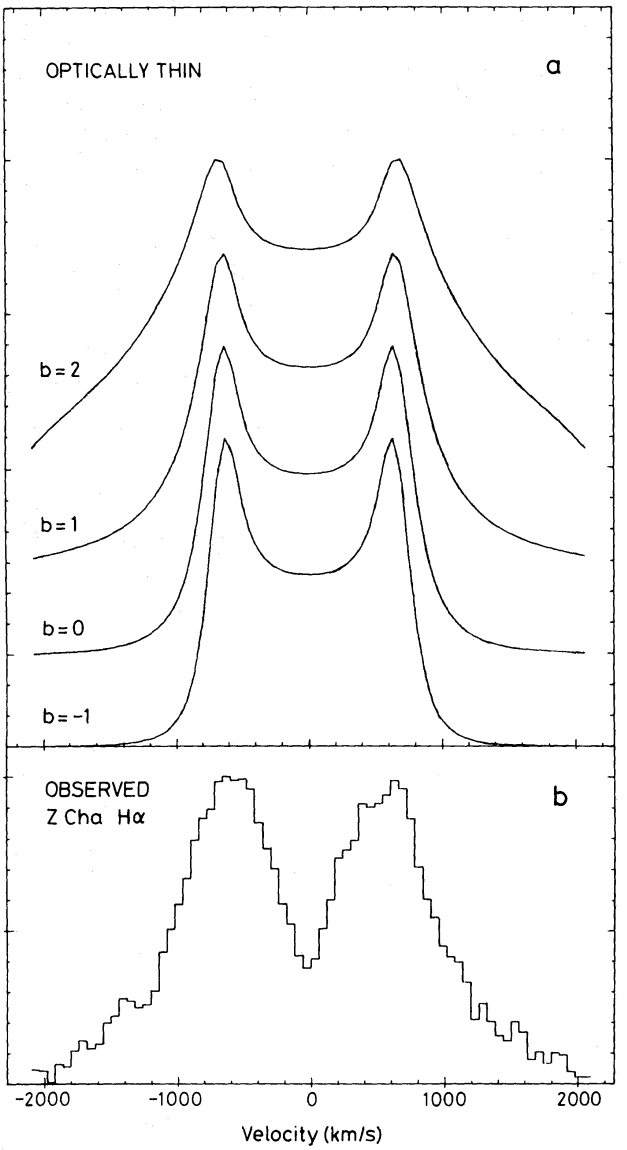

Figure 2. (a) A series of synthetic line profiles for optically thin emission lines formed in a Keplerian accretion disc. The Keplerian velocities at the inner and outer edges of the disc are 2200 and 700 km s^{-1} respectively. The line emissivity varies with radius R as $J \propto R^{-b}$ for different power-law indices b. The profiles are convolved with a Gaussian to simulate the instrumental response (150 km s^{-1} FWHM) and are normalized to a peak value of 10. (b) The Hα line profile of the high-inclination (i=82°) dwarf nova Z Cha in quiescence based on data obtained at the Anglo-Australian Telescope. The instrumental resolution is 150 km s^{-1} FWHM.

Fits of the power-law model to an observed line profile involve two scale parameters and three shape parameters. The scale parameters are the integrated line flux $J \equiv \int F_\nu \, d\nu$ and the velocity separation between the emission peaks, which is $2V_{\rm Kep} \sin i$ at the outer rim of the disc. The power-law index b controls the shape of the profile wings; in velocity space the wings vary roughly in proportion to V^{-2b-5}. The extent of the wings is determined by the velocity $V_{\rm max}$ at the inner boundary of the disc, or equivalently by the ratio $R_{\rm D}/R_{\rm min}$ of the outer to the inner disc radius. Lastly, a local velocity dispersion ΔV and finite instrumental resolution combine to soften the two cusps. The separate effects of these parameters on the global line profile are nicely illustrated by Smak (1981).

Stover (1981) fits the Hβ emission line profile of U Gem using a model with b=1.5, $R_{\rm out}/R_{\rm in}$=22 and $\Delta V = 0.12\, V_{\rm Kep}$. Young *et al.* (1981b) find that a $b \sim 2$ model fits the Balmer

emission lines in HT Cas. They note also a disparity between the rounded peaks of the observed emission lines and the sharp cusps they could expect to see with their high spectral resolution. Smak (1981), analysing published data for six systems, finds power-law indices between 1 and 2.2 and $R_{\rm out}/R_{\rm in}$ in the range 10–50. The consensus of these studies is that the Balmer emission lines in quiescent dwarf novae extend over a large radius range, and that the line surface brightness increases steeply towards the centre of the disc.

The line surface brightness profile $j(R)$ and the shape of the global emission line profile $F(V)$ are closely connected. The possibility of inverting the Abel integral equation that relates the radial emissivity profile to the velocity profile of the line was noted by Huang (1972), and Smak (1981) has reconstructed $j(R)$ from observed line profiles for several systems to check the validity of the power-law model. This one-dimensional Doppler mapping procedure can be extended to a full two-dimensional tomographic reconstruction of $j(R,\theta)$ from emission line profiles $F(V,\phi)$ covering a range of binary phase ϕ.

A simple description of disc emission lines in terms of an isotropic line emissivity $j(R)$ thus offers a satisfying explanation for double-peaked profiles, and provides a flexible framework for interpretation of observations of emission lines from discs. In the next section we show that this description is valid only for optically thin lines and consider how the prescription may be altered to cope with the optically thick case.

3 Local radiative transfer in discs

3.1 THE IMPORTANCE OF SHEAR

We begin our treatment of the local radiative transfer problem by demonstrating the importance of the Keplerian velocity gradient across the finite thickness of the disc. Along an inclined line-of-sight, which traverses a horizontal distance of about $H\tan i$ in passing obliquely through the disc, the Doppler shifts due to the Keplerian orbital motion cover a range given roughly by

$$\Delta V_{\rm D}\sim\frac{H}{R}V_{\rm Kep}\sin i\tan i. \tag{7}$$

One might at first expect this small shift to be of little consequence in a thin disc ($H/R\lesssim 0.05$), except perhaps for very large inclinations ($\tan i\gtrsim R/H$; $i\gtrsim 87°$). Note, however, that the thermal velocity in the disc is

$$V_{\rm th}\sim\frac{H}{R}V_{\rm Kep}, \tag{8}$$

a consequence of hydrostatic equilibrium, in which the disc thickness is determined by a balance between the vertical components of the pressure gradient and the gravity of the central object. Since the transfer of line radiation is affected when $\Delta V_{\rm D}\sim V_{\rm th}$, we can expect shear to influence the local radiative transfer at quite modest inclinations ($\tan i\gtrsim 1$).

We shall assume that the line formation region is a thin layer within which the velocity field may be approximated by a linear shear matched to the local Keplerian flow. Thus we neglect curvature of the streamlines and assume that departures of the velocity field from a pure Keplerian flow are also of order $V_{\rm Kep}(H/R)^2$. The radial velocity of material crossing the inclined line-of-sight at a height Z above the centre of the emission layer is then

$$V_{\rm D}(Z)\simeq V_{\rm D}(0)+\frac{Z}{H}V_{\rm shear}, \tag{9}$$

where H is the thickness of the emission layer, $V_D(0)$ is the mean velocity shift, given by equation (2), and the shear velocity is

$$V_{\text{shear}}=-\frac{2}{3}\frac{H}{R}V_{\text{Kep}}\sin i\tan i\sin\theta\cos\theta. \tag{10}$$

Our neglect of streamline curvature is justified except at very large inclinations ($\tan i\gtrsim R/H$; $i\gtrsim 87°$). Our treatment can cope with an isotropic 'microturbulence', but 'macroturbulence' involving eddy velocities comparable with $V_{\text{Kep}}(H/R)$ and length scales of order H must be excluded.

3.2 THE LINE OPTICAL DEPTH

One important consequence of the Keplerian velocity shear in the emission layer is that the optical depth along different lines-of-sight will depend upon the azimuth θ as well as the inclination i. The optical depth is obtained by integrating the opacity $\varkappa_\nu$ along the inclined line-of-sight:

$$\tau_\nu=\int_{-\infty}^{+\infty}\frac{dZ}{\cos i}\varkappa_\nu. \tag{11}$$

Continuum opacity in the emission layer is assumed to be small in comparison with the line opacity, which is given by

$$\varkappa_\nu=\frac{\pi e^2}{mc}fn(Z)\phi_\nu(Z). \tag{12}$$

Here f is the absorption oscillator strength of the transition, $n(Z)$ is the number density of the absorbing atoms, and $\phi_\nu(Z)$ is the local absorption profile

$$\int_0^\infty \phi_\nu\, d\nu=1.$$

At this point we require information about the vertical structure of the emission layer, since both n and ϕ_ν vary with Z. Vertical hydrostatic equilibrium suggests a density profile of the form

$$n(Z)=n(0)\exp\left\{-\frac{1}{2}\left(\frac{Z}{H}\right)^2\right\}, \tag{13}$$

where the vertical scale height H is related to the thermal speed V_{th} (assumed to be independent of Z) by

$$\frac{H}{R}\sim\frac{V_{\text{th}}}{V_{\text{Kep}}}. \tag{14}$$

We adopt a Gaussian form for the velocity distribution of the absorbers:

$$\phi_\nu=\frac{1}{\sqrt{2\pi}\Delta\nu_{\text{th}}}\exp\left[-\frac{1}{2}\left\{\frac{\nu-\nu_D(Z)}{\Delta\nu_{\text{th}}}\right\}^2\right]. \tag{15}$$

Here the line centre is Doppler shifted from frequency ν_0 to

$$\nu_D(Z)=\nu_0\left\{1-\frac{V_D(Z)}{c}\right\}, \tag{16}$$

and the thermal width of the line is

$$\Delta\nu_{\rm th}=\nu_0\frac{V_{\rm th}}{c} \tag{17}$$

where c is the speed of light.

These Gaussian forms for the distribution of opacity over Z and ν are convenient for our purposes because, in combination with our approximation of the velocity field by a linear shear, they permit us to evaluate the optical depth integral over Z analytically. The resulting expression for the line optical depth is

$$\tau_\nu=\frac{W}{\cos i}\frac{1}{\sqrt{2\pi}\Delta\nu}\exp\left[-\frac{1}{2}\left\{\frac{\nu-\nu D(0)}{\Delta\nu}\right\}^2\right]. \tag{18}$$

Here we express the line strength in terms of the parameter W, which is given by

$$W=\frac{\pi e^2}{mc}f\int_{-\infty}^{+\infty}n(Z)dZ. \tag{19}$$

(For an optically thin line, W is the absorption equivalent width in frequency units.) The largest optical depth occurs at the Doppler-shifted frequency $\nu_{\rm D}(0)$ that corresponds to the orbit velocity of material at the midpoint of the emission layer. The linewidth $\Delta\nu$ in equation (18) is larger than the normal thermal width $\Delta\nu_{\rm th}$ by a factor which depends on both the thickness of the emission layer and the direction (i,θ) from which it is observed:

$$\Delta\nu=\Delta\nu_{\rm th}(1+Q^2\sin^2 i\tan^2 i\sin^2 2\theta)^{1/2}. \tag{20}$$

Here Q is a dimensionless parameter which expresses the ratio of the shear broadening produced by the Keplerian flow to the normal thermal broadening:

$$Q=\frac{3}{4}\frac{V_{\rm Kep}}{V_{\rm th}}\frac{H}{R}. \tag{21}$$

Q is about unity for an emission layer that spans the entire thickness of the disc, as for example in the Williams (1980) and Tylenda (1981) models.

Shear broadening, unlike thermal broadening, is anisotropic. Its angular dependence, indicated in equation (20), is easily understood. The $\sin i$ factor stems from the projection on to the line-of-sight of orbital velocities in the plane of the disc, while $\tan i$ reflects the increased path length through the emission layer at high inclinations. Thus shear broadening vanishes for $i=0$ and dominates for $i\gtrsim 60°$, the transition between these regimes being fairly abrupt.

The $\sin 2\theta$ azimuthal dependence, which has important consequences for the global profiles of optically thick emission lines, is a projection effect. When viewed in the radial direction ($\theta=0,\pi$), the shear broadening is zero because orbital velocities are perpendicular to the line-of-sight. The shear broadening also vanishes for the lines of sight $\theta=\pm\pi/2$, which are tangential to the cylinders of constant radius on which the orbit speed is constant (see Fig. 1a). The local emission line achieves its greatest width when viewed at 45° to the radial and tangential directions.

3.3 THE LINE SURFACE BRIGHTNESS

The (continuum-subtracted) line intensity emerging from the emission layer is

$$I_\nu=I_\nu^{\rm B}\exp(-\tau_{\rm c})\{\exp(-\tau_\nu)-1\}+S_{\rm L}\exp(-\tau_{\rm c})\{1-\exp(-\tau_\nu)\}, \tag{22}$$

where $\tau_{\rm c}$ and τ_ν are continuum and line optical depths through the emission layer, $S_{\rm L}$ is the line

source function in the emission layer, and I_ν^B is the intensity of background radiation, which might arise from an optically thick region behind the emission layer. An assumption implicit in equation (22) is that the line source function S_L is constant in the emission layer. This approximation follows in spirit the LTE models (Williams 1980; Tylenda 1981) in which the line source function is a Planck function evaluated at the local temperature. In a more general situation S_L may be regarded as a representative value of the source function in the emission layer. We shall neglect continuum opacity and background light for the purposes of this paper; they may be included straightforwardly in numerical calculations. The local emission line profile then reduces to $S_L\{1-\exp(-\tau_\nu)\}$ with τ_ν given by equation (18). Fig. 3 provides examples of local line profiles for optically thick and optically thin lines at two different linewidths.

The emission line surface brightness is obtained by integrating the local line intensity over frequency and multiplying by $\cos i$ to account for foreshortening:

$$J=\cos i\, S_L \int d\nu\,\{1-\exp(-\tau_\nu)\}. \tag{23}$$

In the optically thin case, the factor $1-\exp(-\tau_\nu)$ is approximately equal to τ_ν, and the frequency integration consequently gives

$$J_{\text{thin}} \simeq S_L W. \tag{24}$$

Note that optically thin lines emit isotropically; line photons emerge freely from the optically thin emission layer.

In the optically thick case, the local line profile consists of a core region in which the line intensity saturates at the source function and wings in which the intensity falls rapidly to zero. The area under the saturated line profile is therefore well approximated by the product of S_L and the

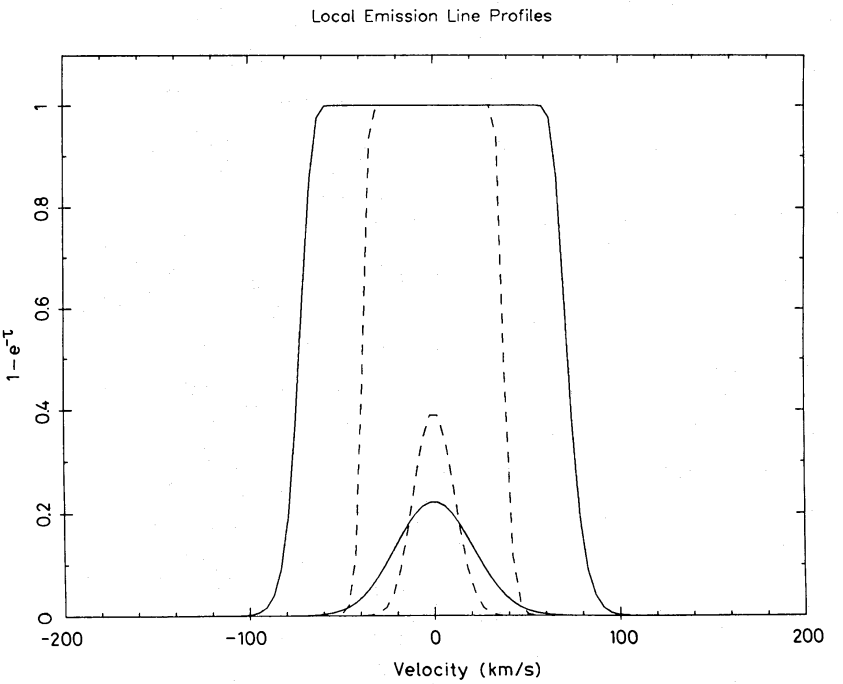

Figure 3. Optically thick and optically thin line profiles for two different velocity widths. The total area under the optically thin line profile is independent of its velocity width. In the optically thick case, the core of the line is saturated and its area increases approximately in proportion to its width. This effect gives rise to anisotropic line emission from shearing media such as the surface of an accretion disc.

width of the frequency interval within which the line optical depth exceeds unity:

$$J_{\rm thick} \simeq \cos i \, S_{\rm L} \Delta\nu (8 \ln \tau_0)^{1/2} \tag{25}$$

where

$$\tau_0 = \frac{W}{\sqrt{2\pi}\Delta\nu \cos i} \tag{26}$$

is the central optical depth of the line.

In sharp contrast with the optically thin case, optically thick line emission is strongly anisotropic. The $\cos i$ factor in (25) accounts for foreshortening of the saturated line intensity. The emissivity is roughly proportional to the local linewidth $\Delta\nu$, which depends upon both inclination and azimuth as a result of the anisotropic shear broadening. Thus the line photons trapped in the optically thick emission line layer tend to leak out close to the orbital plane in the 45° directions along which the Keplerian shear provides a large Doppler shift gradient. The azimuthal variation of the local emission pattern alters the character of the global profiles of optically thick lines from discs, as we shall see in the next section.

4 Discussion

We have seen how a disc's Keplerian velocity field introduces an anisotropic component in the local line broadening. This shear broadening arises because an inclined line-of-sight encounters material moving with different orbital velocities as it passes through an emission layer of finite vertical thickness. The shear broadening increases with inclination, and dominates the normal isotropic thermal broadening at moderately large inclinations ($i \gtrsim 60°$).

Shear broadening is of minor importance for optically thin lines, in which line photons escape freely from the emission line region in all directions, but for an optically thick line the shear broadening generates an azimuthal variation of the line emissivity that modifies the shape of the disc's global line profile. Line photons tend to emerge from an optically thick emission layer in directions along which the Keplerian velocity field of the disc provides a velocity gradient.

The formulae derived in the previous section may be used in a straightforward manner to compute the profiles of optically thick or optically thin emission lines from accretion discs. Line profiles in these two limits are compared in Fig. 4 for a range of inclinations. The emission line profiles fall into several regimes depending on the relative importance of three broadening mechanisms: the orbital broadening $V_{\rm Kep} \sin i$, the isotropic thermal broadening $V_{\rm th} \sim V_{\rm Kep}(H/R)$, and the shear broadening $V_{\rm shear} \sim V_{\rm Kep}(H/R) \sin i \tan i$.

At very small inclinations, $\sin i \lesssim H/R$, the isotropic thermal broadening dominates because the Keplerian orbital velocities in the disc are nearly perpendicular to the line-of-sight. The line profiles are single peaked.

At moderately small inclinations, $(H/R)^2 \lesssim \sin i \tan i \lesssim 1$, orbital broadening produces a double-peaked line profile. Shear broadening is still small in comparison with thermal broadening, and is not yet large enough to cause appreciable azimuthal variation of the line emissivity. Thus the shapes of the optically thick and optically thin line profiles are nearly identical.

At moderately large inclinations, $1 \lesssim \sin i \tan i \lesssim R/H$, shear broadening exceeds the thermal broadening, and the local emissivity of the optically thick line becomes anisotropic. Optically thin line profiles retain their sharp emission peaks separated by a shallow U-shaped valley, while optically thick line profiles develop a deeper roughly V-shaped absorption between broader emission peaks. Note the striking resemblance between the optically thick profile for $i = 82°$ and the observed Hα emission profile of Z Cha given in Fig. 2(b).

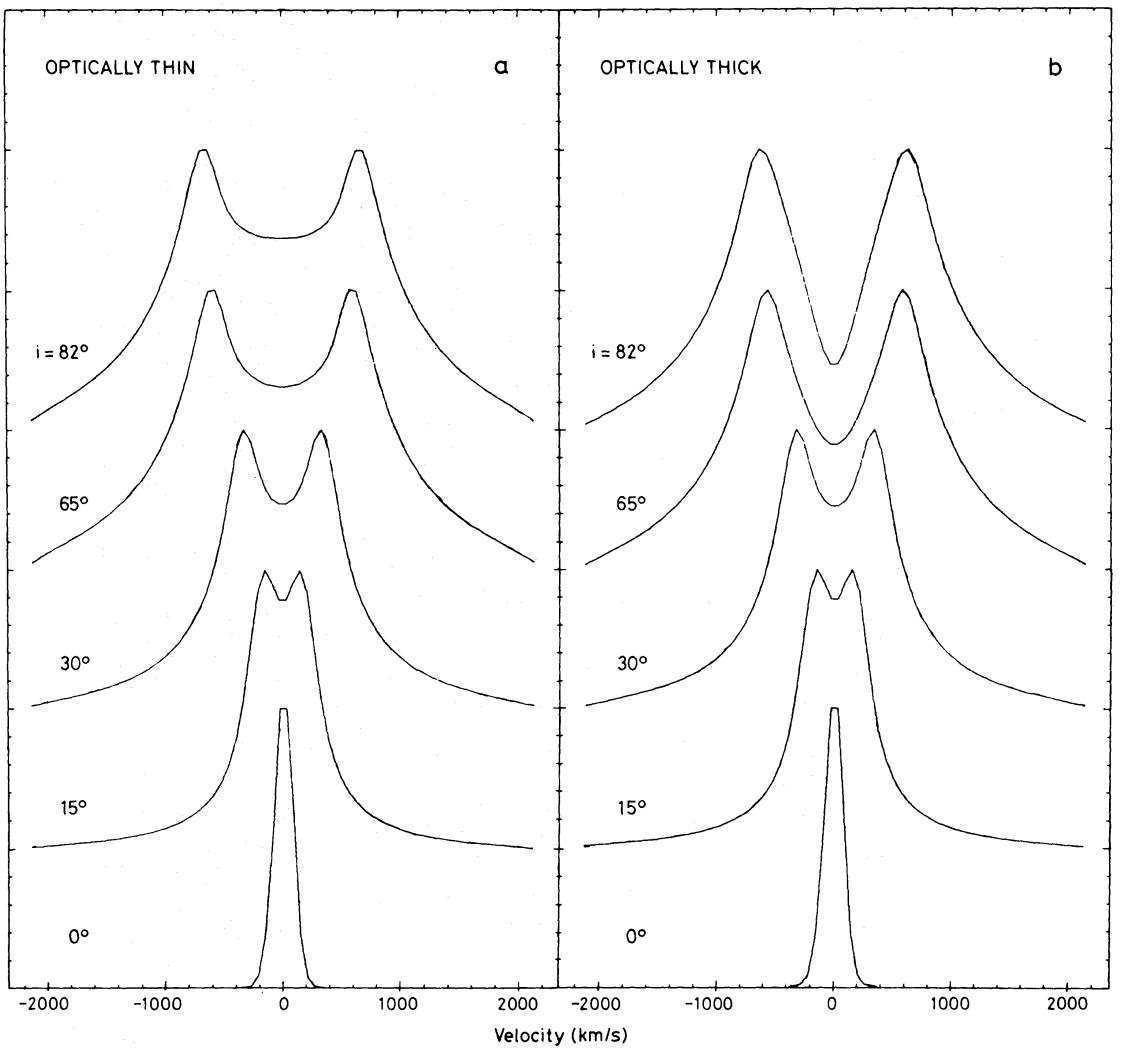

Figure 4. Synthetic line profiles for optically thin and optically thick emission lines covering a range of inclinations. The Keplerian velocities at the inner and outer edges of the accretion disc are 2200 and 700 km s^{-1} respectively. The local line broadening includes an isotropic component due to thermal motions and an anisotropic component due to shear in the Keplerian disc. The line emissivity is $J \propto R^{-1.7}$ for the optically thin case, and the line source function is $S_L \propto R^{-1.2}$ for the optically thick case. The profiles are convolved with a Gaussian to simulate the instrumental response (150 km s^{-1} FWHM) and are normalized to a peak value of 10. Compare the optically thick profile for $i=82°$ with the observed profile in Fig. 2(b).

Finally, at very large inclinations, $\tan i \gtrsim R/H$, lines-of-sight traverse a large radius range in passing through the accretion disc and the approximations of our first-order treatment break down.

In these calculations, we have assumed that the local velocity profile is Gaussian. (A boxcar profile is perhaps a better representation for the saturated local profiles in the optically thick case, but our use of a Gaussian has only a small effect on the spatially integrated line profile.) We assumed $H/R=1/50$ and $Q=1$ at every point on the disc surface. To match the shape of the emission line wings of Hα in Z Cha, we chose $j \propto R^{-1.7}$ for the optically thin model and $S_L \propto R^{-1.2}$ for the optically thick model. [We neglected the azimuthal dependence of $\sqrt{(\ln \tau_0)}$.] The predicted profiles are convolved with a Gaussian to simulate the instrumental resolution (150 km s^{-1} FWHM) and are normalized to a peak value of 10.

We have shown that shear broadening and line saturation are important elements of the line formation process in discs. Our high-inclination optically thick emission line profiles successfully reproduce the Balmer emission line profiles of eclipsing dwarf novae such as Z Cha. Optically thin lines, however, have sharp emission peaks and shallow U-shaped valleys that are inconsistent with the observations.

Several conclusions drawn from analyses within the optically thin formulation are now given a new perspective. The steep radial line emissivity profiles $j(R)$ that have been found by fitting the wings of the observed emission line profiles are interpreted, according to (25), as measurements of the line source function multiplied by the local line width. The rounded emission peaks seen in U Gem (Stover 1981) and in HT Cas (Young *et al.* 1981b) and previously regarded as evidence for large turbulent velocities, implying $H/R \sim 0.12$ at the outer rim of the disc, are now seen to be a natural consequence of shear broadening. Masses derived from analyses of emission line eclipse phenomena (HT Cas, Young *et al.* 1981b; LX Ser, Young *et al.* 1981a; DQ Her, Young & Schneider 1980) may require revision, since the mean radius of disc material at a given radial velocity is different for optically thick lines.

The broad single-peaked emission lines seen in some cataclysmic variable stars remain an enigma. Fig. 4 indicates that the emission peaks should easily be resolved at inclinations as small as 15°, yet in several eclipsing systems (e.g. LX Ser, Young *et al.* 1981a) the emission line profiles are single peaked. Eclipse phenomena demonstrate that the emission line region in these systems is close to the disc plane and rotating with the disc. This would seem to require $H/R \sim 1$ for at least part of the emission line region, or a local line broadening mechanism that does not enter into the vertical hydrostatic equilibrium.

The formulae derived here provide a framework for the interpretation of optically thick and optically thin emission lines from discs in terms of the local characteristics of the emission region. Further analysis of observed line profiles using image reconstruction techniques should soon provide a firm observational basis from which to develop detailed models for line emission from accretion discs.

Acknowledgments

We are indebted to Jim Pringle, Janet Drew and Alison Campbell for helpful comments on a draft of this paper.

References

Clarke, J. T., Capel, D. & Bowyer, S., 1985. *Astrophys. J.*, in press.
Elitzer, M., Ferland, G. J., Mathews, W. G. & Schields, G. A., 1983. *Astrophys. J. Lett.*, **272,** L55.
Gorbatskii, V. G., 1975. *Soviet Astr.–A.J.*, **8,** 680.
Greenstein, J. L. & Kraft, R. P., 1959. *Astrophys. J.*, **130,** 99.
Huang, S., 1972. *Astrophys. J.*, **171,** 549.
Jameson, R., King, A. & Sherrington, M., 1980. *Mon. Not. R. astr. Soc.*, **191,** 559.
Liang, E. D. T. & Price, R. H., 1977. *Astrophys. J.*, **218,** 247.
Marsh, T. R. & Horne, K., 1985. *Mon. Not. R. astr. Soc.*, in preparation.
Rybicki, G. B. & Hummer, D. G., 1983. *Astrophys. J.*, **274,** 380.
Schoembs, R. & Hartman, K., 1984. *Astr. Astrophys.*, **128,** 37.
Schwarzenberg-Czerny, A., 1981. *Acta Astr.*, **31,** 241.
Smak, J., 1969. *Acta Astr.*, **19,** 155.
Smak, J., 1981. *Acta Astr.*, **31,** 395.
Stover, R. J., 1981. *Astrophys. J.*, **248,** 684.
Tylenda, R., 1981. *Acta Astr.*, **31,** 127.

Williams, G., 1983. *Astrophys. J. Suppl.,* **53,** 523.
Williams, R., 1980. *Astrophys. J.,* **235,** 939.
Young, P. & Schneider, D. P., 1980. *Astrophys. J.,* **238,** 955.
Young, P., Schneider, D. P. & Shectman, S. A., 1981a. *Astrophys. J.,* **244,** 259.
Young, P., Schneider, D. P. & Shectman, S. A., 1981b. *Astrophys. J.,* **245,** 1035.